Surface x-ray diffraction from Co/Pt(111) ultrathin films and alloys: Structure and magnetism

S. Ferrer, J. Alvarez, E. Lundgren, X. Torrelles, P. Fajardo, and F. Boscherini*
European Synchrotron Radiation Facility, Boîte Postale 220, 38043 Grenoble Cedex, France
(Received 7 April 1997)

Surface x-ray-diffraction measurements have been done in cobalt ultrathin films (2–12 atomic layers) grown on Pt(111). Cobalt grows, at room temperature, in an imperfect layer-by-layer mode with its own lateral lattice spacing. The packing of the atomic planes is predominantly fcc but it changes to hcp upon annealing to ~450 K. Further annealing to ~550 K results in alloying. Several alloys have been identified with stoichiometries close to the bulk stable phases. Resonant magnetic diffraction experiments in the L_{III} absorption edge of Pt allow one to determine the magnetism of the Pt atoms at the interface. By measuring magnetic crystal truncation rods, it has been found that only the Pt atoms in contact with the Co overlayer are magnetized ($\sim 0.2\mu_B$) being the magnetization of the second Pt layer about ten times smaller. The induced magnetic moment of the Pt interface has been found to depend rather linearly on the thickness of the Co film, similarly to the magnetization of the overlayer. The transformation fcc to hcp of the cobalt stacking results in a ~25% enhancement of the magnetization at the interface. [S0163-1829(97)10039-X]

I. INTRODUCTION

Multilayers based on Co and Pt have attracted enormous interest in the last few years as practical candidates for magneto-optical storage media. The main reasons for this are the observation of enhancements of the Kerr rotations near the plasma frequency of the Pt metal and the perpendicular magnetic anisotropy exhibited by multilayers having a Co thickness of less than about 10 Å.[1] These observations have triggered a number of experimental and theoretical studies that try to elucidate the microscopic origins of these effects. Within the present understanding, it appears that the increasingly large perpendicular anisotropy of the Co orbital magnetic moment when the thickness decreases is the key feature for the perpendicular anisotropy.[2,3] The enhancement of the Kerr rotation would be originated by the exceptionally large spin-orbit coupling in the interface Pt layer compared to other transition metal systems.[4]

The relationship between the magnetic properties of a multilayer or of a thin film and its atomic structure have also been a major field of research producing very interesting findings. To mention some, early experiments suggested already a direct relation between the magnetic anisotropy and atomic sharpness of the interfaces in Co/Au multilayers.[5] The sensitivity of the magneto-optical spectra to the atomic surface *ordering* was evidenced in a Co_3Pt surface ordered alloys grown by MBE (molecular beam epitaxy).[6] Also, $CoPt_3$ thin films were found to exhibit enhanced Curie temperatures compared to the usual bulk alloy, the reason probably being the existence of a miscibility gap in the surface alloys due to some surface effect.[7] Finally, strong magnetic anisotropy was found in hcp cobalt thin films, whereas this was not the case for fcc films.[8]

Motivated by the rich phenomenology exhibited by the thin magnetic films and by the important relations between atomic structure and magnetic properties, we investigated Co/Pt(111) surfaces by performing surface x-ray-diffraction measurements. The technique was employed in two different contexts. From one side, ''normal'' measurements as usually done in surface crystallography provided information on the growth kinetics of the films, on their atomic packing (fcc and hcp), and on the different alloy compositions formed upon annealing. The last question was possible thanks to the large momentum resolution available. These findings are presented in Sec. IV.

From the other side, resonant magnetic diffraction measurements were performed in the L_{III} absorption edge of Pt. As previously obtained surface magnetic results in a Co_3Pt alloy,[9] such experiments allow one to probe the magnetic moment of the Pt atoms induced by the magnetized Co overlayer. From the present measurements it has been found that the magnetism of the interface Pt atoms increases with the thickness of the cobalt films, that the interface Pt magnetism is confined to essentially one atomic layer, the one in contact with the cobalt, that the Pt magnetic moment is slightly larger for overlayer cobalt films with hcp packing than for films with fcc packing, and finally that the Pt interface magnetism is strongly reduced upon surface alloying of the cobalt overlayers. These findings are reported in Sec. V. Section II is devoted to experimental details and Sec. III describes briefly the physics on the resonant magnetic scattering measurements and its suitability to surface magnetism.

II. EXPERIMENTAL DETAILS

The experiments were performed on the Surface Diffraction beamline at ESRF, which has been previously described in detail.[10] A new important development of the beamline not mentioned in Ref. 10 is the insertion of two flat Rh mirrors mounted in a nondispersive geometry after the monochromator, which has reduced the high-order harmonic content in the monochromatic beam by several orders of magnitude. The Pt crystal was of (111) orientation with a miscut angle of less than 0.1°. It was prepared by a large number of sputtering-annealing to 1200 K cycles. The resulting bulk and surface mosaicities were 0.016 and 0.065°, respectively. The cleanliness of the surface was monitored with Auger electron spectroscopy. Occasionally carbon impurities were observed at levels of 0.10 atomic layers. That concentration was estimated by measuring the ratio of the

carbon and Pt peak at 237 eV and multiplying by 0.6.[11]

The crystal was not described with the standard cubic basis but instead with a hexagonal basis $\mathbf{a}_1$, $\mathbf{a}_2$, $\mathbf{a}_3$ with $\mathbf{a}_1$ and $\mathbf{a}_2$ in the surface plane (a_1 and a_2 are equal to the nearest-neighbor surface distance $a_0/\sqrt{2}$) and $\mathbf{a}_3$ perpendicular to the surface ($a_3=\sqrt{3}a_0$). The corresponding reciprocal lattice vectors are directed along three axes H,K,L with H and K in the surface plane making an angle of 120° and L normal to the surface. With this basis, bulk Bragg reflections are found at $(H,K)=(1,0)$, $L=1,4,7,\ldots$ and $(H,K)=(0,1)$, $L=2,5,8,\ldots$. Diffraction data were collected with photon energies close to the L_{III} Pt absorption edge at fixed angles of incidence ranging from the critical angle for total external reflection (0.3°) to 2°. Diffracted intensities at (H,K,L) were measured by rocking the crystal around its normal, integrating the resulting angular scans and applying the appropriate correction factors [12]. The diffracted intensity from the sample was cleaned from fluorescent background by means of a highly oriented graphite crystal acting as crystal analyzer that was mounted in a two-circle goniometer installed in the detector arm of the diffractometer. With this setting, the signal-to-background ratio in the minimum of the a crystal truncation rod when the photon energy was set to the L_{III} Pt absorption edge was about 10. The detector was a commercial NaI scintillator.

Magnetic measurements were performed by applying an external field of 1.2 kOe maximum intensity parallel to the surface. It was created by a permanent magnet installed inside the UHV chamber. It could be rotated by a step motor acting on a rotary feedthrough, so as to invert the direction of the field from vertical pointing upwards to downwards. Normally the measurements were performed by collecting the diffracted intensity with the field upwards for a time interval around 15 or 30 s, then the field was inverted and the intensity was measured during the same time interval. This operation was repeated 16 or 32 times to perform temporal averaging. Typically this resulted in statistical error bars of around 0.5 to 1×10^{-3} in the asymmetry ratio. The measurements required a very good beam stability since otherwise spurious asymmetry values were encountered. This was controlled by measuring the asymmetry ratio of an ancillary intensity monitor that was away from the sample and not affected by magnetic fields. Cobalt deposits were done with a water-cooled electron bombardment evaporator. During depositions the pressure was in the low 10^{-10}-mbar range.

III. RESONANT MAGNETIC DIFFRACTION: APPLICATIONS TO SURFACE MAGNETISM

The interaction of x rays with atoms possessing a magnetic moment gives rise to the magnetic scattering process that was brought to experimental evidence in 1972 (Ref. 13) and since then has been employed to the study of magnetism in solids. The cross section of the process is, however, so small compared with ordinary Thomson scattering cross sections that its application to investigate surface magnetism is out of the question even with the intense beams generated by the third-generation synchrotron radiation source as ESRF. The discovery of the resonant exchange scattering effect,[14] which results in a large enhancement (several orders of magnitude) of the magnetic scattering cross section, made the possibility of applications to surface problems realistic.

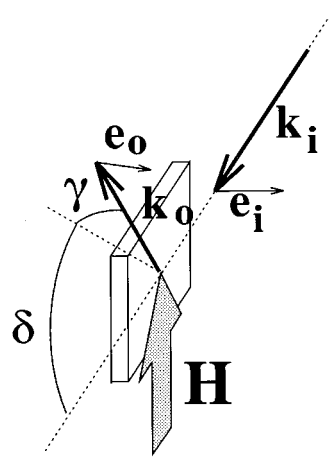

FIG. 1. Schematic layout of the geometry of the experiment. The sample surface lies in a vertical plane and is illuminated by the incoming wave vector $\mathbf{k}_i$ with polarization $\mathbf{e}_i$. The direction of the scattered wave vector $\mathbf{k}_0$ is determined by the angles γ and δ. **H** denotes the applied magnetic field that may be directed upwards or downwards.

The resonant exchange scattering process occurs when the photon energy is tuned to an absorption edge of an atom resulting in strong electric multipole transitions from the core level to the empty states at the Fermi level. If these states are exchange split then the process is sensitive to the magnetism of the absorbing atom.[15] In order to have a strong enhancement, the scattering has to involve low-order multipole transitions and unfilled atomic or narrow-band states. Pt atoms with their relatively narrow $5d$ bands fulfill these conditions and therefore display intense resonant effects.[16]

Our experiments were performed by setting the photon energy at the L_{III} absorption edge of Pt (11.564 keV). Under these conditions, the scattering amplitude contains, in addition to the usual Thomson charge scattering f_0, significant contributions of the dispersive (f') and absorptive parts (f'') and the resonant magnetic term. The scattering geometry used in our experiments is depicted in Fig. 1. The surface of the sample lies in a vertical plane and is illuminated by a grazing x-ray beam. The direction of the scattered beam is defined by two angles as indicated in the figure: the exit angle γ relative to the plane of the surface and the angle of in-plane scattering δ determined by the projection to the surface plane of the outgoing and incoming wave vectors. Under this geometry, if the sample is magnetized in the vertical direction, recalling that the incoming polarization is horizontal, one has for the scattering amplitude in units of r_0, the electron radius[15,16]

$$f=\cos\gamma(f_0+f'-if'')+a_{\mathrm{res}}, \tag{1}$$

$$a_{\mathrm{res}}=\frac{i+x}{1+x^2}\,(-n_p\cos\gamma-i\epsilon n_m\sin\gamma\cos\delta). \tag{2}$$

n_p accounts for the white line at the absorption edge. Its numerical value is taken from Ref. 16 to be 4.3. ϵ may take

the values 1 and -1 depending on the up or down orientation of the magnetization. x determines the relative energy deviation from resonance:

$$x=\frac{(E_f-E_i)-h\nu}{\Gamma/2}. \tag{3}$$

E_f-E_i is the transition energy, $h\nu$ the energy of the photon, and Γ the width of the core level taken from Ref. 16. The most important quantity is n_m, which is defined as the difference in the transition probabilities of dipolar transitions, from the core level to the Fermi level, involving changes of angular momentum Δj_z of 1 and -1. The nonzero value of n_m in a magnetic atom arises from the spin splitting in the conduction band originated by the exchange interaction. In a somewhat loose sense, n_m may be visualized as being proportional to the magnetic moment of the resonant atom.

Expressions (1) and (2) are valid at zero incidence angles, which is a good approximation for our experiments. For arbitrary incidence angles the appropriate formulas[15,16] have to be used. As may be seen from Eqs. (1) and (2), the diffracted intensity, which is proportional to $|f|^2$, will contain terms with odd parity in ε; therefore the asymmetry ratio

$$R=\frac{I\uparrow-I\downarrow}{I\uparrow+I\downarrow} \tag{4}$$

will be different from zero at the resonance energy ($x\approx 0$) where it exhibits a maximum. Away from resonance R decreases and the function $R(x)$ has a line shape that resembles a Lorentzian. Its detailed form has been discussed in Ref. 16.

The application of the resonant effect to surface magnetism is based on two facts. First, if the angle of incidence of the x-ray beam is equal to or smaller than the critical angle for total reflection, the penetration of the beam in the sample is very small (~ 50 Å), resulting in a surface sensitivity within this length scale. This surface sensitivity can be relaxed by simply increasing the angle of incidence. This technique has been recently applied to study temperature-dependent disordering effects.[17] Second, one may apply the usual methods of surface crystallography, namely, the measurements of the intensities along crystal truncation rods[12] to have surface sensitivity at the level of one atomic plane. The method consists in measuring the intensities $I_{HK}(L)$ at fixed values of H and K and continuously varying values of L (the direction of the surface normal). Away from the HKL values where Bragg conditions are fulfilled, the intensities are extremely sensitive to the surface since the amplitudes of consecutive HKL planes in the bulk of the crystal have opposite phases and thus cancel. The measured $I_{HK}(L)$ intensities provide information on the structure of the surface along the L direction. Similarly, by measuring the dependence of the asymmetry ratio along a crystal truncation rod, $R_{HK}(L)$, one may obtain detailed information on the magnetic structure of the atoms at resonance conditions, i.e., the distribution of magnetic moments along the surface normal with a sensitivity down to one atomic plane.

As shown in Eq. (2), εn_m has to be different from zero to have a magnetic resonant effect that originates a nonzero asymmetry ratio. In more detail, this implies that the projection of the magnetic moment of the resonant atom along the field direction does not have to be zero. In practice it may occur that for perpendicularly anisotropic surfaces the intensity of the in-plane external field is not enough to completely rotate the magnetization to the film plane. In such a case, only the projection of the magnetization in the surface plane would be sensed by the asymmetry ratio of Eq. (4). Therefore if one has to extract from the asymmetry ratio numerical values of n_m that can be related to magnetic moments at saturation, one has to make sure that the ferromagnetic film is indeed saturated in the plane.

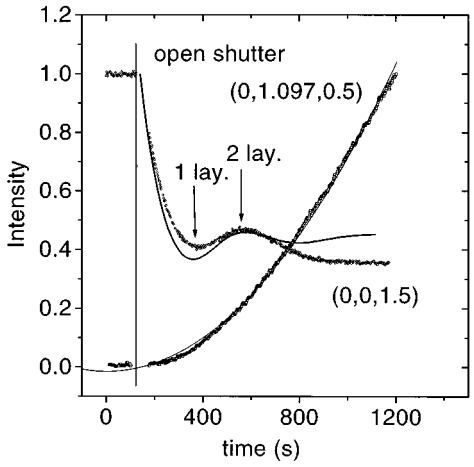

FIG. 2. Temporal evolution of the diffracted intensities at (0,0,1.5) and (0,1.097,0.5) during deposition of cobalt at room temperature, the continuous curves are calculated (see text).

IV. STRUCTURAL RESULTS

A. Growth of cobalt on Pt(111)

The monitoring of film growth was done by recording the temporal evolution of the diffracted intensity at (0,0,1.5). At this reciprocal space location, as H and K are zero, the intensity is only sensitive to the atomic coordinates along the direction of the surface normal. The L value was chosen since as it lies just in between two consecutive Bragg reflections (at $L=0$ and 3), the surface sensitivity is very large since the diffracted amplitudes from the (111) planes in the crystal cancel as described above.

As shown in Fig. 2, the intensity displays a maximum after an initial decay. The continuous line is the result of a calculation obtained by considering the appropriate atomic factors and a simple model of imperfect layer-by-layer growth. The local maximum at $t\sim 600$ s corresponds to a two atomic layers thick film. Although the calculated curve fits the data only moderately well, it is useful enough to illustrate the degree of imperfection of the growth; for example, the calculation shows that after deposition of three atomic layers, the first layer is complete, the second has a coverage of ~ 0.95, the third of ~ 0.6, the fourth of ~ 0.25, and the fifth of ~ 0.10. In other words, three levels or more are coexisting on the surface during growth. This observation is in agreement with the previously published STM work by Grutter and Durig[18] in which a multileveled surface was observed.

By letting H and (or) K be different from zero, one may probe the atomic coordinates along the surface plane. The nearest-neighbor distance of Co atoms in a cobalt crystal is

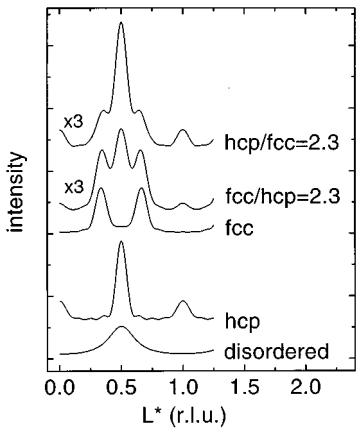

FIG. 3. Diffracted intensities vs perpendicular momentum transfer calculated for different packing of eight (111) planes. The bottom curve is for a disordered packing; the second for a hcp packing, the third for a fcc packing, the fourth for a mixture of disordered, fcc, and hcp packing with predominance of fcc, and the top curve corresponds to a mixture of disordered, fcc, and hcp with a dominance of hcp.

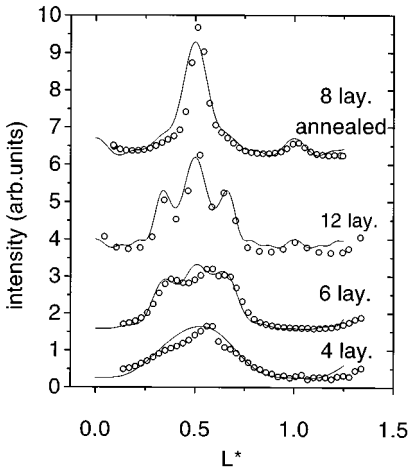

FIG. 4. The data points are integrated intensities at $(H,K)=(0,1.097)$ as a function of perpendicular momentum transfer for cobalt films of different thickness. The three lowest data sets are for deposition at room temperature. The top one was obtained after annealing to ~ 450 K a film of 8 atomic layers. The continuous curves are fits using the Guinier model.

9.7% smaller than that of a Pt crystal. If cobalt grows on top of Pt with its own lattice spacing one should have in reciprocal space satellite peaks at $(H\times 1.097,\ K\times 1.097)$. To investigate this possibility, the temporal evolution of the intensity at (0,1.097,0.5) was measured (the value of L was chosen for sensitivity reasons and it is somewhat arbitrary). As is depicted in the figure, the scattered intensity shows an increasing slope with time. This can be understood on the basis of general arguments by realizing that the intensity is proportional to the square of the diffracted amplitude, which in turn is proportional to the concentration of cobalt coverage, which increases linearly with time. Therefore the intensity has been adjusted with a parabolic function as $I\propto(t-t_0)^2$, where t_0 represents a possible temporal lag in the appearance of the structure. The continuous curve fits the data with $t_0=2.6$ s, which is almost 100 times shorter that the time required to deposit one layer (224 s). This shows that cobalt grows from the very start with its own lateral spacing and not in pseudomorphism with the Pt substrate. This observation differs from that of Refs. 18 and 19, which suggest that the first deposited layer of cobalt grows with the lateral spacing of the substrate but it agrees with recent low-energy electron diffraction studies.[20]

An important aspect of the growth of the cobalt films concerns the stacking of the (111) planes since platinum is fcc and cobalt is hcp (at room temperature). In addition, the reduced atomic mobility of the adatoms will likely result in structural disorder. The atomic structure of cobalt films of different thickness has been investigated by measuring the diffracted intensity at (0, 1.097) for different values of L. We will analyze these structural data following the ideas of Guinier,[21] which will be described briefly. The L axis has been rescaled for convenience to the bulk hcp lattice parameter by letting $L^*=1$ to correspond to $2\pi/(c/2)$ with c being the Co lattice constant (4.07 Å).

The Guinier model evaluates the diffracted intensity from a set of N planes characterized by an interplane correlation function, as a discrete $2N$ term Fourier series with coefficients corresponding to the magnitudes of the correlations of planes situated at different distances. For a perfect hcp stacking, the correlation function shows maxima at 2,4, . . . interlayer spacings and zeros at 1,3, ... For a perfect fcc the maxima are at 3,6, . . . and the zeros at 1,2,4,5, ... A disordered packing sequence that is neither hcp nor fcc will be characterized by nearest-neighbor plane correlations only; i.e., there is zero probability that the nearest-neighbor planes of plane type A will be plane type A, but there is a 50% chance that the second neighbor will be plane type A, etc.

In reciprocal space, the hcp packing gives peaks at $L^*=0.5$ and 1, the fcc at $\frac{1}{3}$, and the disordered at $L^*=0.5$. If, in addition, the two twin fcc packings (ABC and ACB) are equally probable, another intense maximum at $L^*=2/3$ has to be expected.

Figure 3 shows several examples of that model for $N=8$ atomic planes. The three lowest curves correspond respectively to disordered, hcp, and fcc packings, respectively. The two topmost curves are a linear combination of the intensities of the lowest curves. Their respective weights (disordered/hcp/fcc) are 0.5/0.35/0.15 and 0.5/0.15/0.35.

The model is very simple since it ignores any possible relaxations or rumpling in the planes and more complicated types of disorder. However, as will be shown below, it provides a reasonable description of the experimental data and it allows one to estimate the proportions of different types of stacking.

Figure 4 shows the experimental data for cobalt films of different thickness and calculations using the above model. The data points are integrated intensities of rocking scans through the surface normal corrected with the appropriate geometrical factors. The number of data points in the experiment of 12 layers is less than in the others but in this case two equivalent rods were measured and averaged.

The fits to the data indicate that in all cases the disordered component is the most important one. Its relative weight ranges from 75 to 85%. The data from 4 and 6 layers have

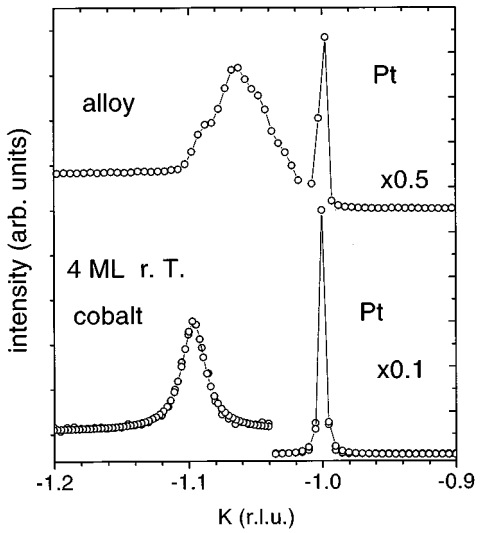

FIG. 5. Transverse scans in the vicinity of $(H,K)=(0,-1)$ for a 4-atomic-layer films as deposited at room temperature (bottom) and after alloying (top). Alloying causes a decrease in intensity of the sharp Pt peak at $K=-1.00$ and a shift and broadening of the cobalt peak originally at $K=-1.097$.

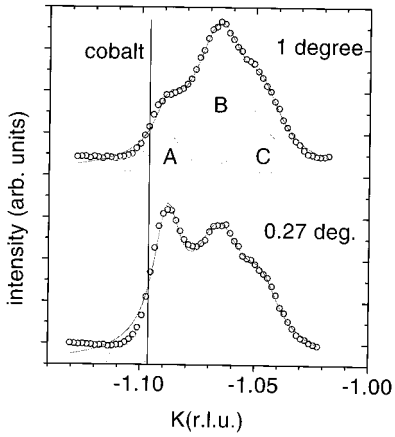

FIG. 6. Transverse scans of the cobalt diffracted peaks after alloying. Three alloy peaks are resolved. The bottom curve is taken at a greater grazing angle of incidence than the top one, revealing that alloy *A* is on the surface.

0% hcp contribution. For 12 and 8 layers (annealed) the hcp to fcc percentage ratios are 8/17 and 20/0, respectively.

Close inspection of the data in Fig. 4 shows that the central maximum in the cases of 4 and 6 layers is not at $L^*=0.50$ as expected but shifted towards higher L^* values. This shift causes the two fcc derived peaks located at both sides of the central peak to have different intensities. This is an indication of a change in interlayer spacing. It has been introduced in the calculations by varying the spacing of the planes in the disordered contribution of the intensity. The curves on the figure correspond to an expansion of 3%. The expansion may be a consequence of the disorder on the stacking uncorrelated to lateral strain as has been suggested previously.[35]

In summary, although the films show in all cases an important stacking disorder, they are predominantly fcc for low thickness. Moderate annealing causes a transformation from fcc to hcp packing but it does not eliminate the stacking disorder.

B. Surface alloying

Deposition of cobalt films at room temperature with thickness in the range 4–8 atomic layers, results in ordered cobalt regions with characteristic linear dimensions of about 132 Å, evaluated as $2\pi/\Delta K$ where ΔK is the full width at half maximum (FWHM) of a cobalt reflection measured at low L values. Annealing to $\sim$450 K for a few minutes induces a sharpening of the reflections, which corresponds to an increase of the ordered regions to 235 Å typically. Further annealing causes a more pronounced modification of the cobalt reflections as illustrated in Fig. 5. The bottom curve shows the platinum and cobalt and reflections at (1, -1,0.48) and (1,-1.097,0.48), respectively. Annealing to $\sim$600 K for 10 min modifies the diffracted intensity as illustrated in the top curve. The intensity of the Pt reflection has decreased by a factor 7, that of the cobalt has increased by a factor of about 2, and, more important, the position of the cobalt reflections is shifted towards the Pt and exhibits a significant broadening. These observations are indicative of Co-Pt alloying. Figure 6 shows the cobalt reflection in more detail. The top curve was recorded at an angle of incidence of the x rays about 3 times larger than the critical angle of total external reflection, therefore the penetration of the x rays is much larger than that of the bottom curve that was taken at the critical angle (0.27°). The data have been fitted with three Lorentzian peaks as shown in the figure. The fit parameters are the following. The positions of peaks *A*, *B*, and *C* are, respectively, -1.088, -1.066, and -1.047. The respective widths are (in reciprocal lattice units) 0.014, 0.028, and 0.019. The different peak positions are indicative of different in-plane lattice parameters, which correspond to different surface alloys. Alloy *A* is concentrated in the topmost surface planes and it is the richest in cobalt since its lattice parameter is closer to the cobalt lattice spacing than that of alloys *B* and *C*. Annealing to temperatures above $\sim$600 K causes an additional alloy component to form. Figure 7 shows the temporal evolution of the diffracted intensity from an 8-layer-thick film. The top curve was taken after raising the sample temperature to 600 K. It displays the alloy components *B* and *C* discussed above. Alloy *A* is not apparent in the scan perhaps because the pure cobalt peak masks it. The bottom scan is taken a few minutes later. The intensities from the pure cobalt and from the alloys *B* and *C* have disappeared and a new surface alloy has been formed, giving an intensity at $K=-1.017$.

The diffracted intensities of the different surface alloys along the surface normal differ considerably as illustrated in Fig. 8, which shows L scans from a film of 8 layers under different circumstances. The bottom curve corresponds to the room temperature film and it displays the triple peak structure discussed above, characteristic of disordered and fcc packing. Annealing at $\sim$450 K causes the transformation to hcp with the disappearance of the peaks at both sides of the central one. Alloy *B* displays the main maximum at $L=1.94$ and alloy *C* at $L=2.09$.

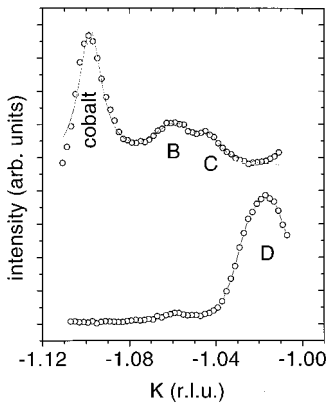

FIG. 7. Transverse scans of the cobalt diffracted peaks. Top curve: the alloying is not complete since intensity coming from nonalloyed cobalt is apparent. Bottom curve: complete alloying of the cobalt. The peak labeled D closely corresponds to the $CoPt_3$ stoichiometry (see text).

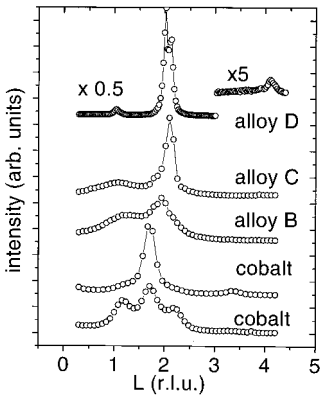

FIG. 8. L scans along the cobalt rods for different situations. The two lowest curves are for nonalloyed cobalt films either as deposited at room temperature (bottom) where the film is predominately fcc, or after transformation to hcp (second curve). The three topmost curves correspond to the different alloys discussed in the text.

Alloy D exhibits sharper peaks in L than those of alloys B and C. They are located at $L=1.026$ and at two and four times the above value. Whereas the intensity distributions of alloys B and C have a nonstraightforward interpretation, the intensity of alloy D is easily understandable with general arguments. All the L scans on the figure have H and K coordinates close to 1 and -1, respectively. The nearby crystal truncation rod of the Pt substrate at $(1,-1,L)$ exhibits bulk Bragg reflections at $L=2,5,\ldots$. If the Pt substrate had crystallites with the twin fcc packing, one would also observe intensity at $L=1,4,\ldots$. This is not the case for the Pt crystal but it is what occurs in the surface alloy D. The main peak at $L\sim 2$ results from the stacking sequence of the Pt substrate. The small peaks at $L\sim 1$ and 4 are a consequence of the existence of some regions of twinned packing in the alloy. Furthermore, the positions of the peaks in the L axis indicate that alloy D has an interlayer distance along [111] 2.6% shorter than that of the Pt crystal. The in-plane lattice spacing for this alloy is 1.7% shorter than that of the Pt as indicated by the position of the maximum of the bottom curve in Fig. 6. The difference between the above values is considered to be close to the experimental error bars and we believe that alloy D is a cubic fcc alloy with an a_0 parameter about 2% shorter than that of Pt.

The in-plane lattice spacings of the different alloys may be used to determine the relative concentrations of platinum and cobalt. Figure 9 shows the lattice constant of different alloys as a function of the Pt content. The squares have been taken from the work of Dhamani[22] and correspond to bulk alloys. The circles correspond to the different surface alloys identified in our work. The line that fits the data allows one to determine the different Pt concentrations (%), which result to be: $x_A=11.8$, $x_B=28.5$, $x_C=44.5$, and $x_D=76.4$. The compositions of alloys B, C, and D are, respectively, close to the ones of $PtCo_3$, PtCo, and Pt_3Co, which are thermodynamically stable phases.[23] However, a word of caution is necessary. The above correlation between stoichiometry and lattice constant is based on bulk alloys and may not be completely correct in thin films due to the possible existence of strain. Previous studies[35] on transition-metal multilayers (Co/Au and Co/Cu) found lateral stains of around 1%. If this were the case in our Co/Pt films, it would result in an uncertainty of $\sim 8\%$ on the Pt concentrations depicted in Fig. 9. Nevertheless, the fact that cobalt grows with its own lattice spacing when it is deposited at room temperature (Sec. IV A) may be taken as an indication of a rather negligible strain in this system.

C. Platinum crystal truncation rods

In order to investigate the possible relaxations caused by the cobalt overlayers on the Pt topmost atomic layers, the rods $(1,0,L)$ and $(0,1,L)$ of the Pt substrate were measured with and without cobalt overlayers. The results from the clean Pt agreed with those of Ref. 24 in the sense that no significant relaxations were found on the Pt topmost planes. This situation was not modified by the cobalt deposition at room temperature since the Pt rods were unaltered except for an attenuation factor.

V. RESONANT MAGNETIC SURFACE DIFFRACTION MEASUREMENTS

A. Interfacial Pt magnetism of films deposited at room temperature

To bring to evidence the resonant exchange process on the Co/Pt system, the photon energy was scanned through the L_{III} absorption edge of Pt and the asymmetry ratio was measured as explained in Sec. II. Figure 10 shows the results for a cobalt film of four atomic layers in thickness. The measurements were taken at $(HKL)=(1,0,2.85)$, which is near the crystal truncation rod (CTR) minimum at $L=2.5$ and the surface sensitivity is large. As it may be seen, a clear resonant behavior is apparent. The maximum value of the asymmetry ratio is around 3×10^{-3} and the width of the resonance is 6.5 eV, which results from the convolution of the energy width of the $2p_{3/2}$ Pt core level and the energy resolution of the Si(111) monochromator. The continuous curve is a fit to the data with the formulas in Sec. III. The Pt crystal was assumed to have magnetized atoms only in the topmost atomic plane in contact with the cobalt film (the reason for

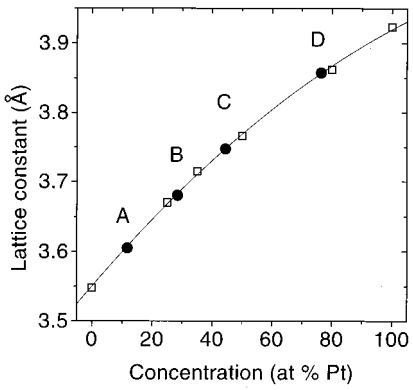

FIG. 9. Dependence of the lattice constant with the Pt concentration for different PtCo alloys. The open squares are from the work of Dahmani (Ref. 22) for bulk alloys. The black circles correspond to the different surface alloys identified in this work.

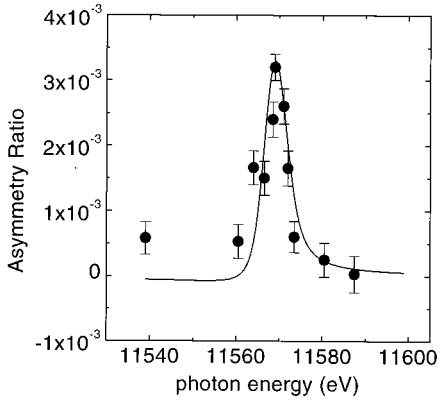

FIG. 10. Dependence of the magnetic asymmetry ratio as a function of the photon energy at the vicinities of the L_{III} absorption edge of Pt for a film of cobalt of approximately 4 atomic layers deposited at room temperature on the Pt substrate. The resonance at the Pt absorption edge is a consequence of the magnetism of the Pt atoms at the interface.

this will be clear below) and no atomic relaxations on the Pt topmost layer were included in the calculation. Also, the energy spread ΔE of the incoming x-ray beam from the monochromator was included in the calculation by convoluting the asymmetry $R(x)$ (see Sec. III) with a Gaussian distribution with a FWHM of $\Delta E = 4.7$ eV. With these assumptions, there is only one parameter to be adjusted, namely, n_m, the magnitude of the induced magnetism of the Pt atoms. The resulting value is -0.13 for the data in the figure (the minus sign comes from the sign conventions in the atomic factor and may be ignored for the discussion).

As explained in Sec. III, the distribution of magnetized Pt atoms may be determined by measuring magnetic crystal truncation rods. Figure 11 shows the results of the $(1,0,L)$ rod with $0.5 < L < 4.5$ for a surface consisting in a film of eight atomic layers of cobalt on the Pt substrate. The measurements give $R = 0$ at $L = 1$ and 4 where Bragg conditions of the Pt crystal are satisfied, indicating that the bulk of the Pt crystal is not magnetized. This is to be expected since the ferromagnetic overlayer will magnetize most likely only the Pt atomic planes at its vicinity since Pt is a nonmagnetic material. However, R is different from zero between $L = 1$ and 4, which indicates the existence of magnetized Pt atoms at the interface. The measured R values show a broad, unstructured distribution extending several Brillouin zones, suggesting a narrow distribution of magnetized Pt atoms along the surface normal. To fit the data, the formulas of Sec. III were employed and the nonzero energy spread of the monochromatic beam was taken into account. The calculated $R_{HK}(L)$ values are indicated by the continuous curve in the figure. In this case two adjustable parameters were included in the calculation: n_{m1} and n_{m2}, for the two topmost Pt atomic planes, respectively. The results are $n_{m1} = -0.52 \pm 0.02$ and $n_{m2} = -0.05 \pm 0.02$. This indicates that only the Pt atomic plane in contact with the cobalt films is significantly magnetized since the magnetization of the next atomic plane is about 10 times smaller. Similar measurements to those in the figure were performed for cobalt films of different thickness. The results were identical to those in Fig. 11 except for a proportionality factor.

The numerical value $n_{m1} = -0.52$ is close to the -0.43 ± 0.1 that was found in a previous work[9] on a single crystal of Co_3Pt for the Pt atoms at the surface of that crystal. In that case the Pt atoms at the surface had on the average five cobalt nearest neighbors whereas in the thin film they have only three. The relationship between n_m and the magnetic moment of the Pt atoms is not obvious but on the basis of general arguments it may be assumed that a sort of proportionality has to exist for a given type of atom and a given absorption edge. This is so since the different probabilities of dipolar transitions to the majority and minority empty spin states at the Fermi level have to be closely related to the difference in density of states between both spin bands, which is proportional to the magnetic moment of the atoms.

The measured magnetic moments of Pt atoms in CoPt alloys is in the range $(0.25-0.45)\mu_B$ depending on the degree of order of the alloy and on the composition.[23,25] Previous measurements[9,16] of resonant scattering in CoPt and in Co_3Pt gave $-0.9 < n_m < -0.8$ for bulk Pt atoms. Therefore as an empirical rule of thumb one may take that $n_m = -2.4$ corresponds to 1 Bohr magneton. This would give $\sim 0.2\mu_B$ and $\sim 0.02\mu_B$ for the magnetic moment of the topmost Pt layer and second layer, respectively in the Co/Pt interface. The above values may be compared with those of Ref. 26 where the magnetic moments of Pt atoms in different CoPt multilayers were calculated from a first-principles muffin-tin orbital method. These authors found spin magnetic moments in the range $(0.17-0.20)\mu_B$ for the Pt atoms in contact with the cobalt in very good agreement with our results (the orbital magnetic moments were much smaller). However, they also found that the second Pt layer had a magnetic moment about two or three times smaller that of the first one, which is in variance with our results. Another theoretical work based on local-density total-energy calculations[27] obtained $0.38\mu_B$ for the magnetic moment of Pt atoms in contact with the cobalt and a strong decrease of the induced magnetization similar to ours. Spin-polarized photoemission experiments[28] in Pt/Co interfaces reveal the existence of magnetic interface states with Pt $5d$ character that appear to be confined at the interface and do not extend towards the bulk. Our results may also be compared with the x-ray absorption measurements of Schutz *et al.* on Co/Pt multilayers.[29] They esti-

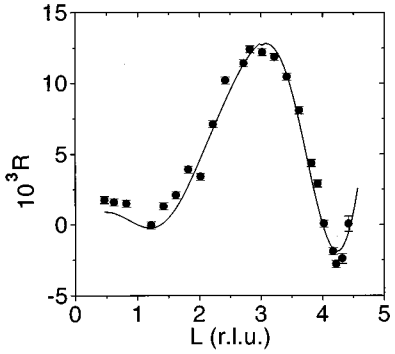

FIG. 11. Dependence of the asymmetry ratio at resonance with the perpendicular momentum transfer for a film of 8 atomic layers of cobalt on the Pt substrate. The continuous curve is a fit to the data that arises from essentially one atomic layer of magnetized Pt at the interface.

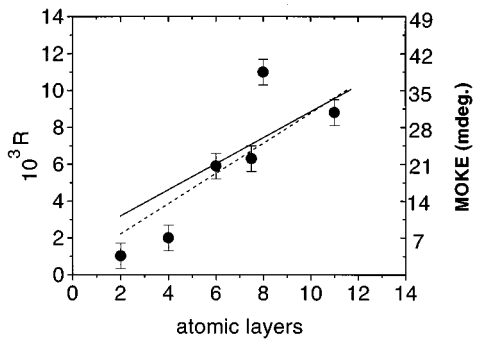

FIG. 12. Dependence of the asymmetry ratio at resonance with the thickness of the cobalt film deposited at room temperature. The right ordinate axis schematizes the results of the Kerr measurements of Ref. 30.

mated a distribution of the magnetic moments of Pt atoms of 0.15, 0.06, and $0.03\mu_B$ for the first, second, and third Pt layers, respectively. The magnitude of the magnetic moment of the Pt layer in contact with the cobalt film is in agreement with our results but the decay of the magnetic moment is smaller than what we found. We believe that our results on the distribution of the magnetic moment are more accurate and reliable since they are obtained from crystallographic analysis of the diffracted (magnetic) intensity.

As the magnetic moment of the Pt atoms is induced by the magnetic field created by the cobalt overlayer, which is magnetized to saturation with the externally applied magnetic field, it is reasonable to assume that the magnetization of the interface Pt layer will be proportional to that in the ferromagnetic overlayer. In this case the magnitude of the asymmetry ratio of the Pt interface atoms could be used as a probe for the magnetization of the cobalt. In order to test this hypothesis, the asymmetry ratio of Pt was measured for different thicknesses of the cobalt overlayer. Figure 12 shows the results. The measurements were done at $(HKL)=(1,0,2.85)$. The incoming angle of incidence was the critical angle for total reflection. The measurements of different thickness were taken under identical conditions. After each measurement the sample was sputter annealed and a new fresh cobalt deposit was done at room temperature. As it may be seen R increases rather linearly with the cobalt thickness in the range 2–11 atomic layers. The figure also shows schematically as lines the results of Kerr measurements of McGee *et al.*[30] for a cobalt wedge grown on Pt(111). The continuous and dashed lines represent respectively the polar Kerr rotations and ellipticities. As the Kerr signals measure the average magnetization of the cobalt overlayers, the similarity in the trends of the asymmetry ratio and Kerr rotations when the thickness of the cobalt film increases may be taken as evidence that the asymmetry ratio is a probe of the magnetization of the overlayer. It is well known that the Curie temperature of very thin magnetic films may be substantially lower than that of the bulk materials.[31] Although, to our knowledge, no measurements have been done for the Co/Pt(111) system, it seems likely that the rather linear increase in Fig. 12 is a consequence of the improved magnetic order at room temperature due to the increasingly higher Curie temperatures of the films.

B. Effects of the temperature on the interface magnetism

As discussed in Sec. IV annealing of the cobalt films to $\sim$450 K results in a fcc to hcp packing transformation. In addition, the dimensions of the ordered cobalt domains increase substantially. We investigated the influence of these effects on the magnetic asymmetry ratio of Pt. Figure 13 depicts the results of measuring the asymmetry ratios at $(HK)=(1,0)$ and $0.5<L<4.3$ for an 8-atomic-layer film deposited at room temperature (bottom data) and the same film after a moderate annealing (top data). The continuous curves are fits to the data with two adjustable parameters n_{m1} and n_{m2} as in Sec. V A. The results are respectively -0.36 ± 0.015 and -0.03 ± 0.015 for the predominantly fcc film (bottom curve) and 0.45 ± 0.04 and -0.12 ± 0.05 for the predominantly hcp film. Although the error bars of the measurements are rather large, it appears that the annealing of the films originates an increase of about 25% of the asymmetry ratio of the interface atoms probably due to an increased magnetism in the overlayer. Whether this increase is due to the hcp packing or to the increase in the dimensions of the ordered cobalt domains has to be elucidated.

Note that the numerical values of R in the bottom data of Fig. 13 are lower than these of Fig. 11 by about 2×10^{-3} whereas both measurements are from an 8-atomic-layer film grown at nominally the same conditions. The measurements in Figs. 11 and 13 were taken with a time interval of several months between them. The deposition rate in Fig. 13 was about 20% larger than that of Fig. 11. These sorts of irreproducibilities have also been found in other situations and are believed to be due to noncontrolled differences in the growth conditions or substrate quality.

Finally we investigated the effect of alloying in the interface magnetism. This was achieved by growing a film of cobalt at room temperature and measuring the asymmetry after annealing at increasingly higher temperatures. Figure 14 depicts the results for a film of about four atomic layers in thickness. The measurements were taken at $(HKL)=(1,0,2.84)$. As it may be seen again, there is a moderate increase in the interface Pt magnetism during the transformation of the film packing to hcp. However, at about 520 K, which coincides with the initiation of the alloying as discussed in Sec. IV B, the asymmetry ratio drops rapidly to zero.

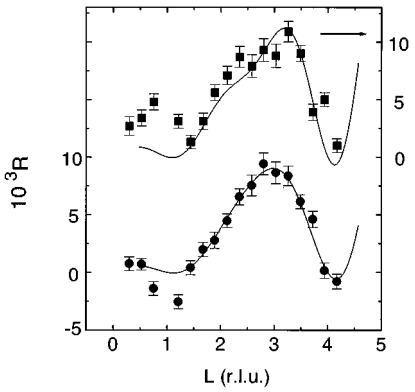

FIG. 13. Magnetic crystal truncation rods (1,0,L) for an 8-atomic-layer film of cobalt as deposited at room temperature on the Pt substrate (bottom) and after an anneal to ~450 K to convert the film to hcp.

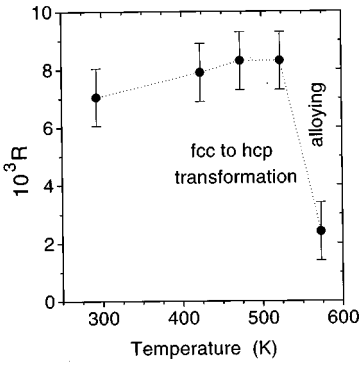

FIG. 14. Evolution of the asymmetry ratio measured at (0, −1,2.84) of a film of 4 atomic layers upon annealing. Alloying at ~520 K causes a drastic reduction of the interface Pt magnetism.

One possible reason for this is the following. Previously published[32,33] work in thin films of Pt/Fe, Pt/Co, and grown with MBE, demonstrates that thermal treatments to ~800 K cause the films to form alloys with some degree of chemical ordering. As a result, the films develop pronounced perpendicular magnetic anisotropy and large coercivities (~4 kOe for Fe/Pt, Ref. 32). Although our thermal treatment are to lower temperatures than those of Refs. 32 and 33 (our films are much thinner), it is very likely that something similar occurs upon alloying. In that case, it could occur that the coercivity in the ultrathin alloys discussed in Sec. IV B were larger than the external applied field used in the experiments (1.2 kOe) preventing magnetic saturation, which would result in very small values of the asymmetry ratio. Similar results on strong perpendicular anisotropy have been found in disordered surface $CoPt_3$ alloys.[34]

Other experiments were performed that tend to confirm the above explanation. Magnetic resonant measurements at the L_{III} edge of Pt were done for the thin film of alloy with composition near $CoPt_3$ discussed in Sec. IV B. The ''bulk'' reflection (1,0,4) and some equivalents to it were measured giving, at resonance, $R=12.0\pm0.3\times10^{-3}$; from this value and that of the structure factor of the (disordered) alloy, we evaluated $n_m(CoPt_3)=-0.56\pm0.05$. This would correspond to a magnetic moment of the Pt atoms of ~0.56/2.4 $=0.23\mu_B$ which is a lower value than one would expect on the basis of previous neutron diffraction measurements,[25] which resulted in $\mu_{\mathrm{Pt}}=0.45$ for disordered alloys. The above value should correspond to $n_m=-1.08$, which resembles that from our previous measurements in bulk Co_3Pt (Ref. 9) ($n_m=-0.9$) and to that of Ref. 16 for CoPt ($n_m=-0.8$). Therefore, on the basis of this argument, it appears that the low value of n_m in the thin film of $CoPt_3$ alloy, arises because the film is not magnetically saturated.

VI. SUMMARY AND CONCLUSIONS

Cobalt films with thickness in the range 2–12 atomic layers, deposited at room temperature on a Pt(111) surface, have been investigated with x-ray diffraction. The film growth has been monitored with measurements of the specularly reflected beam in an antiphase condition and it has been found to consist of an imperfect layer-by-layer mode with three or more atomic levels. The lateral spacing is the corresponding one of cobalt bulk crystal but the interplanar distance is expanded 3%. A simple model to analyze the stacking of the (111) planes of cobalt based on the different correlations among the planes has been applied and it has been found that although the films have substantial stacking disorder, they exhibit fcc packing at small thickness. When the thickness increases to ~12 atomic layers, some hcp packing is detected. Annealing of the films to ~450 K causes the transformation of fcc to hcp packing and an increase in the ordering of the cobalt overlayer. Further annealing to ~550 K induces surface alloying. Several alloys have been identified by measuring their in-plane lattice spacing. Most of them have stoichiometries close to those of bulk stable phases.

Resonant magnetic diffraction measurements at the L_{III} absorption edge of Pt were performed to investigate the magnetism of the Pt atoms induced by the cobalt. This was done by measuring the asymmetry ratio for two opposite orientations of an externally applied magnetic field at different locations in reciprocal space. Measurements of the asymmetry along a crystal truncation rod reveal that the Pt magnetism at the interface reduces to essentially one atomic layer, the one in contact with the cobalt overlayer, which has a magnetic moment of $\sim0.2\mu_B$ being the magnetic moment of the next layer about ten times smaller. The dependence of the asymmetry ratio with the thickness of the cobalt overlayer was found to exhibit a rather linearly increasing behavior similar to that found, by optical techniques, in the saturation magnetization of the overlayer.

The fcc to hcp transformation that occurs upon annealing causes a ~25% increase of the interface Pt magnetism. The possibility that this is due to the change in crystal structure and (or) to the increased dimensions of the ordered cobalt domains that result after annealing has to be elucidated. Alloying of the films reduces drastically the Pt asymmetry at the interface probably due a large increase of perpendicular anisotropy.

*On leave from INFN, PO Box 13, I-00044 Frascati, Italy.
[1] W. B. Zeper, F. J. A. M. Greidanus, P. F. Garcia, and C. R. Fincher, J. Appl. Phys. **65**, 4971 (1989).
[2] D. Weller, Y. Wu, J. Sthor, M. G. Samant, and B. D. Hermsmeier, Phys. Rev. B **49**, 12 888 (1994).
[3] D. Weller, J. Sthor, R. Nakajima, A. Carl, M. G. Samant, C. Chappert, R. Megy, P. Beauvillain, P. Veillet, and G. A. Held, Phys. Rev. Lett. **75**, 3752 (1995).
[4] G. Y. Guo and H. Ebert, Phys. Rev. B **51**, 12 633 (1995).
[5] F. J. A. den Broeder, D. Kuiper, A. P. van de Mosselaer, and W. Hoving, Phys. Rev. Lett. **60**, 2769 (1988).
[6] G. R. Harp, D. Weller, T. A. Rabedeau, R. F. C. Farrow, and M. F. Toney, Phys. Rev. Lett. **71**, 2493 (1993).
[7] P. W. Rooney, A. L. Shapiro, M. Q. Tran, and F. Hellman, Phys. Rev. Lett. **75**, 1843 (1995).
[8] D. Weller, G. R. Harp, R. F. C. Farrow, A. Cebollada, and J. Sticht, Phys. Rev. Lett. **72**, 2097 (1994).
[9] S. Ferrer, P. Fajardo, F. de Bergevin, J. Alvarez, X. Torrelles, H. A. van der Vegt, and V. H. Etgens, Phys. Rev. Lett. **77**, 747 (1996).
[10] S. Ferrer and F. Comin, Rev. Sci. Instrum. **66**, 1674 (1995).
[11] S. Ferrer and H. P. Bonzel, Surf. Sci. **119**, 234 (1982).
[12] For a review see I. K. Robinson, in *Handbook of Synchrotron Radiation*, edited by G. Brown and D. E. Moncton (Elsevier Science Publishers B. V., Amsterdam, 1991), Vol. 3.
[13] F. de Bergevin and M. Brunel, Phys. Lett. **39A**, 141 (1972).
[14] D. Gibbs, D. R. Harsman, E. D. Isaacs, D. B. Mc Whan, D. Mills, and C. Vettier, Phys. Rev. Lett. **61**, 1241 (1988).
[15] J. P. Hanon, G. T. Trammell, M. Blume, and D. Gibbs, Phys. Rev. Lett. **61**, 1245 (1988).
[16] F. de Bergevin, M. Brunel, R. M. Galera, V. Vettier, E. Elkaim, M. Bessiere, and S. Lefebvre, Phys. Rev. B **46**, 10 772 (1992).
[17] G. M. Watson, D. Gibbs, G. H. Lander, B. D. Gaulin, L. E. Berman, Hj. Matzke, and W. Ellis, Phys. Rev. Lett. **77**, 751 (1996).
[18] P. Grutter and U. T. Durig, Phys. Rev. B **49**, 2021 (1994).
[19] M. Galeotti, A. Atrei, U. Bardi, B. Cortigiani, G. Rovida, and M. Torrini, Surf. Sci. **297**, 202 (1993).
[20] R. Baudoing-Savois (private communication).
[21] *X Ray Diffraction in Crystals, Imperfect Crystals and Amorphous Bodies*, edited by A. Guinier (Dover, New York, 1994).
[22] C. E. Dahmani, these Universite Louis Pasteur, Strasbourg, 1985.
[23] M. C. Cadeville, C. E. Dahmani, and F. Kern, J. Magn. Magn. Mater. **54–57**, 1055 (1986).
[24] G. Grubel, K. G. Huang, D. Gibbs, D. M. Zehner, A. R. Sandy, and S. G. J. Mochrie, Phys. Rev. B **48**, 18 119 (1993).
[25] F. Menzinger and A. Paoletti, Phys. Rev. **143**, 365 (1966).
[26] G. Y. Guo and H. Ebert, Phys. Rev. B **51**, 12 633 (1995).
[27] R. Wu, C. Li, and A. J. Freeman, J. Magn. Magn. Mater. **99**, 71 (1991).
[28] W. Weber, D. A. Wesner, D. Hartman, and G. Guntherodt, Phys. Rev. B **46**, 6199 (1992).
[29] G. Schutz, S. Stahler, M. Knulle, and P. Fischer, J. Appl. Phys. **73**, 6430 (1193).
[30] N. W. E. McGee, M. T. Johnson, J. J. de Vries, and J. aan de Stegge, J. Appl. Phys. **73**, 3418 (1993).
[31] F. Huang, M. T. Kief, G. R. Mankey, and R. F. Willis, Phys. Rev. B **49**, 3962 (1994).
[32] B. M. Lairson and B. M. Clemens, Appl. Phys. Lett. **63**, 1438 (1993).
[33] A. Cebollada, D. Weller, J. Sticht, G. R. Harp, R. F. C. Farrow, R. F. Marks, R. Savoy, and J. C. Scott, Phys. Rev. B **50**, 3419 (1994).
[34] M. Maret, M. C. Cadeville, W. Staiger, E. Beaurepaire, R. Poinsot, and A. Herr, Thin Solid Films **275**, 224 (1996).
[35] F. L. Lamelas, H. D. He, and R. Clarke, Phys. Rev. B **43**, 12 296 (1991).